www.czasopisma.pan.pl PAN POLSKA AKADEMIA NAUK www.journals.pan.pl

Arch. Metall. Mater. **68** (2023), 3, 1171-1175

DOI: https://doi.org/10.24425/amm.2023.145490

A. SZEWCZYK[1*], M. FARYNA[1], A. WÓJCIK[1], W. MAZIARZ[1], R. CHULIST[1]

PRECISE ORIENTATION CONTROL OF SINGLE CRYSTALLINE NiMnGa-BASED ALLOYS BY IN-SITU EBSD ANALYSIS

The article presents a precise method for the orientation process of NiMnGa-based single crystals. For this method, a scanning electron microscope equipped with an EBSD camera and a heating stage allowing temperatures exceeding 873 K was used. The orientation process was carried out in both the high-temperature austenite phase and in the room-temperature martensite phase. The facilities allowed for determining the orientation of a single grain of austenite at elevated temperatures as well as the orientation of particular martensitic variants at room temperature. A practically perfect cubic orientation was obtained in the austenitic case with a deviation of about 1° while the samples oriented in the martensitic phase deviated from the desired orientation by 4.5-5.2°. Additionally, the training process of single crystals was carried out in order to show the influence of the orientation process on twinning stress.

Keywords: Orientation; monocrystal; EBSD; austenite; martensite

1. Introduction

The NiMnGa alloys are classified as intelligent materials with a shape memory effect due to the fully reversible thermoelastic martensitic transformation occurring during cooling/heating between two phases, i.e. high-temperature austenite and low-temperature martensite. In addition, these alloys can develop a giant reversible magnetic field-induced strain (MFIS) in the martensitic state. So far, the Ni_2MnGa Heusler alloys close to the stoichiometric composition yield the largest MFIS. The single crystalline form of the material (single crystal term used with respect to the austenite state) shows length changes of the order of 6-12% (depending on the crystal structure) for moderate magnetic fields of about 0.4 T at frequencies of the order of 1 kHz [1-7]. Adjusting the microstructure of Ni-Mn-Ga alloys by magneto-mechanical treatments is essential to obtain a well-defined microstructure i.e. to reduce the number of variants and to decrease the twinning stress for practical applications [8-21]. The training process, as the last step in the preparation procedure of Ni-Mn-Ga alloys, consists of multi-axis compression and is necessary to obtain MFIS in Ni-Mn-Ga single crystals [22-31]. Nevertheless, the precondition for larger MFIS and low twinning stress is a proper <001>(100) orientation expressed in the so-called parent-based coordinate system (CS) [32-34]. In other words, this orientation provides the highest theoretical strain at the lowest possible stress. This is due to the optimization of the Schmid factor for the (101) twin planes as well as the maximum shear stresses that operate on the above-mentioned planes.

Studying the orientation relationship between austenite and martensite in non-modulated Ni-Mn-Ga single crystals [35-36] the Authors revealed a strong asymmetric distribution of martensitic variants with respect to austenite in self-accommodate state. Based on the in-situ measurements it was shown that a single austenitic grain may transform into 24 different tetragonal variants. Combining the microstructural and crystallographic orientation information a hierarchy of twin boundaries was found [36]. This specific sequence results in a hierarchy within the martensite variant formation itself affecting the final orientation of particular martensitic variants. Further investigations on the orientation relationship between austenite and martensite have shown two characteristic arrangements of martensitic variants in Ni-Mn-Ga single crystals. Two groups of variants misoriented with respect to each other either by 6° or 12.2° were demonstrated in [36]. The first group is composed of macro-variants that do not follow twin relations due to nanotwinning and are associated with that rigid body rotation while the other group consists of minor variants which satisfy the twin relations perfectly. Additionally, it has been confirmed that the so-called orthogonal

[1] INSTITUTE OF METALLURGY AND MATERIALS SCIENCE, POLISH ACADEMY OF SCIENCES, 25 REYMONTA STR., 30-059, KRAKÓW, POLAND

* Corresponding author: a.szewczyk@imim.pl

shear process leads to the removal of conjugation boundaries by coordinated secondary twinning on a macro scale. It has to be pointed out that the given mechanism [37] is fully consistent with the asymmetric distribution of martensitic variants reported in works and it helps to explain the asymmetric distribution of martensitic variants in Ni-Mn-Ga single crystals.

Furthermore, the study on the same orientation relationship but with trained single crystals showed that the orientation relationship between austenite and martensite is not always constant and can vary in an orientation range depending on the volume fraction of particular variants. In the case of the single variant state, the main tetragonal axes match perfectly with that of cubic austenite showing that the rigid body rotation which takes place upon cooling to self-accommodate is completely revoked during the training procedure [36]. It also suggests that the training process, which consists of successively compressing mostly cuboid samples along two or three main axes leading to a single variant state, can be considered, to some extent, as a reverse shear process of martensitic transformation in which the associated rigid body rotation is restored. It is important to emphasize, that the papers [35,36] provide results questioning the completeness of theoretical models such as Bain, Kurdjumov-Sachs, Nishiyama-Wassermann and Pitsch and also other models for single crystalline Ni-Mn-Ga alloys which show the symmetric distribution of martensitic variants with respect to orientation of austenite. In simple terms, the training procedure that leads to one-variant state in martensite can be considered as a process that reverses the individual rotations obtained as a result of the aforementioned transformation. This means that the main austenitic axes coincide with the tetragonal or orthorhombic axes of the single martensitic variant of martensite. This also implies that the main monoclinic axes are very close to the orthogonal austenite axes. Based on this implication, the final orientation of the trained single variant of martensite should be consistent with the austenitic orientation. Therefore in this contribution, the orientation of single crystalline materials was cut in two ways; one was based on the austenite orientation and the other orientation was from the average of all the martensitic variants.

2. Experimental

$Ni_{50.2}Mn_{28.3}Ga_{21.5}$ polycrystalline alloy was obtained by induction melting in an argon atmosphere of elements with purity >99.95. The obtained ingot was re-melted three times due to homogenization. Then the modified Bridgeman method was used for growing a single crystal rod of dimension 28 diameter and 100 mm long with an induction furnace under vacuum conditions in order to avoid any reaction during melting. For the sample orientation process, EBSD measurements were performed using a high-resolution field emission FEI FEGSEM Quanta 3D equipped with an EBSD Genesis TSL detector. Additionally, to induce the austenitic phase and conduct in-situ analysis a Murano 525 heating stage manufactured by Gatan was used. Samples for EBSD measurements were cut by a spark erosion machine from an as-grown ingot and prepared roughly on abrasive papers, then they were polished on a canvas with slurries, and finally, they were electropolished using a mixture of perchloric acid (1/10) and ethanol (9/10) cooled to 285 K using a current of 35 V for 5 seconds. In addition, the training process was carried out on own design testing machine with 1 KN load cell at room temperature under compressive stress up to 30 MPa at a strain rate of $10^{-3}s^{-1}$ and consisted of successively compressing the sample along two axes to achieve one type of a twin. Further cutting, after EBSD measuring and proper rotation of the samples, were carried on the same machine, with respect to the very first cut (one of the edges of the obtained sample). The specimen during cutting, was mounted on a special goniometer, which ensures angle rotation accuracy to one degree.

3. Results and discussion

For the verification of the hypothesis presented in the introduction part, orientations of sixteen single crystals were determined, using two approaches i.e. in the austenite and martensite phase. The measurements were conducted at room temperature (low-temperature martensite phase) and at increased temperatures in the range of 328 K to 763 K (high-temperature austenite phase).

Fig. 1 shows a typical self-accommodated microstructure for $Ni_{50}Mn_{30.5}Ga_{19.5}$ alloy with a tetragonal martensite crystal structure. This map shows various martensitic variants as well as colonies formed as a result of the self-accommodation process. It should be noted that the mentioned variants were formed from one austenitic orientation and measured prior to the training process.

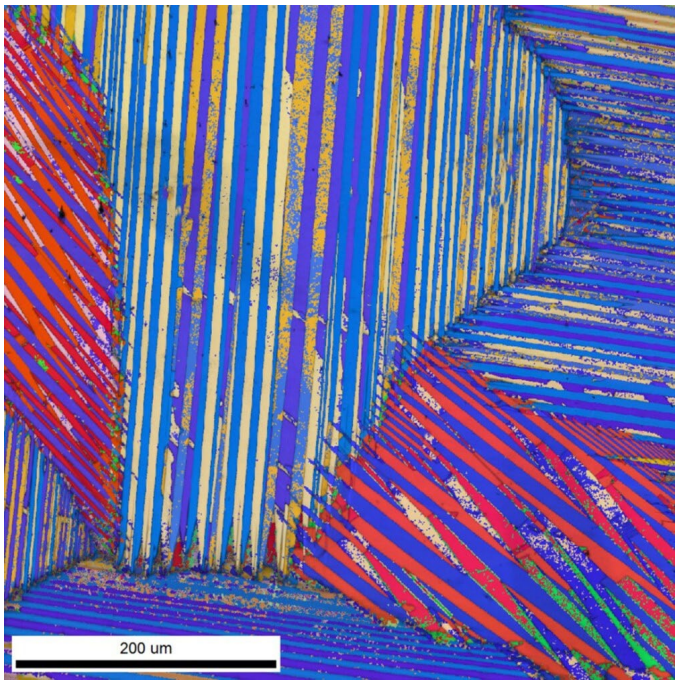

Fig. 1. EBSD mapping of self-accommodated state in $Ni_{50}Mn_{30.5}Ga_{19.5}$ single crystal

The orientations of eight single crystals were measured at room temperature using the methodology presented above. The next eight of the tested single crystals were measured above the reverse transformation temperature i.e. in austenite. In the case of a multivariate martensite system, the average orientation of all measured variants was computed for cutting out the samples.

Fig. 2 shows the sequence of rotations made along the three main axes A3, A1, and A2 (austenitic phase) to bring the crystalline CS into the sample CS, i.e. the external reference system. Using the following sequence of rotations, i.e. rotation of the sample about the axis A3 by 3° (-), then about the axis A1 by 2° (-) and the axis A2 by 12° (-), they were cut out and then reoriented to confirm the <001>(100) orientation.

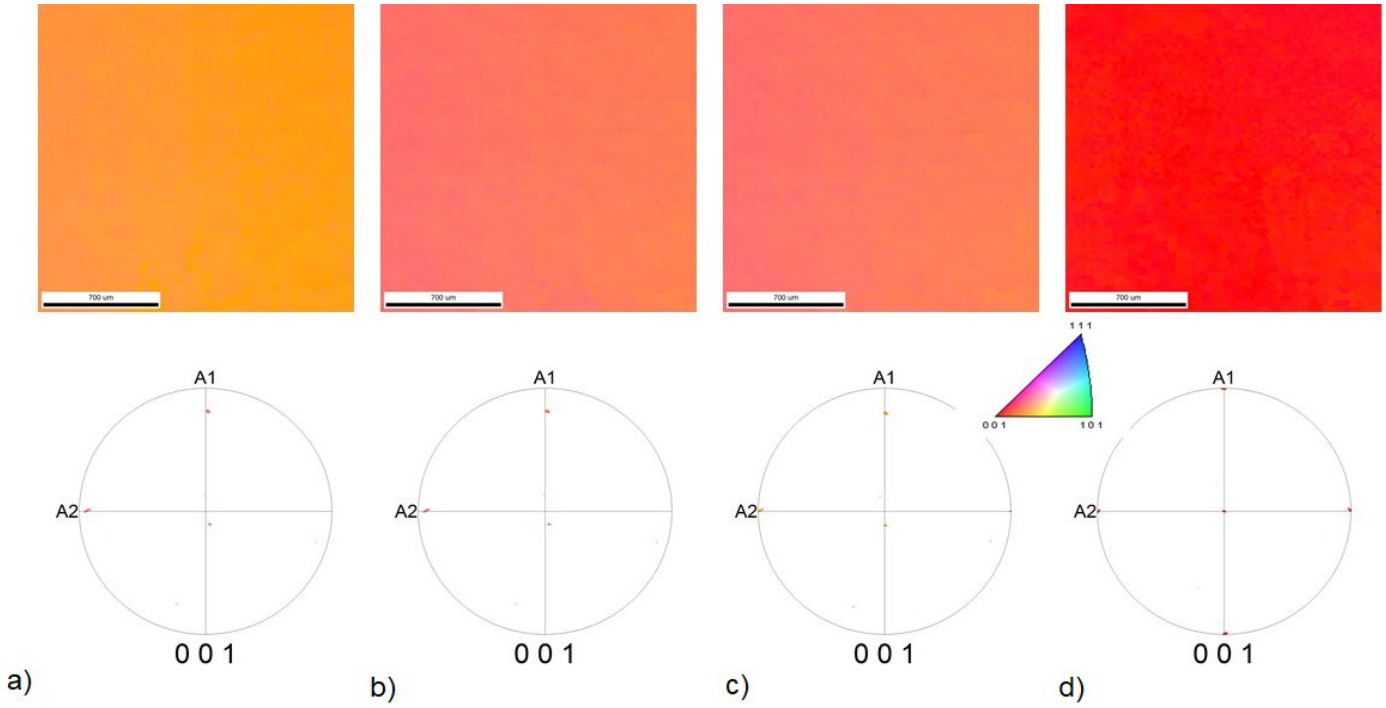

Fig. 2. EBSD maps of the 10M NiMnGa alloy recorded at the temperature of 343 K in the austenite phase showing the steps in the orientation process of single crystals a) initial orientation, b) rotated by A3 axis, c) rotated about A1 axis and d) rotated about A2 axis

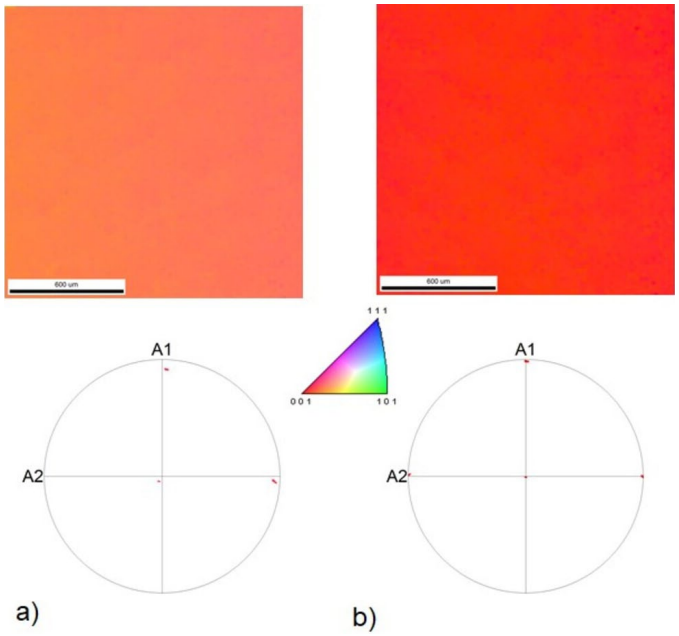

Fig. 3. (a) Superposition of (110) and (001) pole figures in the tetragonal system (both planes represent planes of the (001) type for a cubic system) for single variant of martensite after cutting using room temperature measurements with deviation ~6°and (b) for a sample cut in the austenitic phase (343 K) showing deviation ~1°

Using the same approach, the orientation process and cutting of the samples in a martensitic phase were made assuming the average orientation of all martensitic variants.

Fig. 3 presents two cases with a deviation close to the mean for the measured 8 single crystals in martensite and 8 in austenite. For clarity, they are depicted along with EBSD maps showing the deviation from the <001> orientation colored according to the inverse pole figure with the red color designated as <001>.

Fig. 2 presents the same convention in order to show the progressive development of single crystal orientation on the way to perfect cubic orientation. The mean deviation from the cubic orientation in the case of orientation of single crystals in the austenitic phase was 1.2°, while materials oriented in the martensitic phase were characterized by a deviation from the ideal cubic orientation of about 4.5°. The above-mentioned deviation from the <100> orientation is also visible on EBSD maps using the so-called inverse pole figure color coding with reference to the A3 sample direction, where the orientations closest to <001> are red in accordance with the colors of the basic triangle.

In the next step, the oriented and cut samples were subjected to compression tests along the longest edge ($1 \times 2.5 \times 10$ mm^3) in order to determine the level of twinning stress. The compres-

sion along the longest dimension was chosen because of the lowest friction contribution and the most reliable determination of the twinning stress level.

Fig. 4 shows four stress-strain curves of NiMnGa 10M single crystals with the same chemical composition and geometry between samples. Two of them were cut using the orientation determined in the martensitic phase (deviation at the level of 5.2°; red curve and 4.5°; reddish curve), and the other two others were cut in the austenite phase (about 1° deviation)). Significant differences in the twinning stress level have been observed. As can be seen, single crystals oriented and cut using the orientation measurement in the austenitic phase, are characterized by a lower twinning stress of about 1.2-1.4 MPa (mean stress from the plateau area). On the other hand, single crystals that have been oriented and cut based on measurements at room temperature, i.e. in the martensitic phase, were characterized by twinning stress amounting to 2.1 MPa and 2.7 MPa. In the case of other single crystals, similar relationships were noticed, but due to differences in chemical composition, they were not taken into account in the direct comparison. Changing chemical composition which also changes the crystal structure was intended to develop a universal orienting method independently of the martensite type.

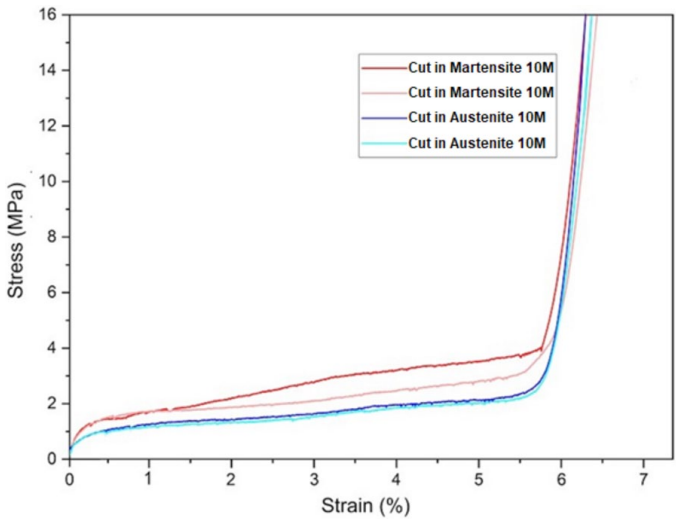

Fig. 4. Stress-strain curves for 4 different $Ni_{50}Mn_{29}Ga_{21}$ single crystalline samples with a 10M crystal structure of the same chemical composition cut in the martensite phase (red) and austenite phase (blue)

4. Conclusion

An important preliminary conclusion of the study is that measurements of single austenite orientations provide much more precise control for cutting single crystals as compared to measurements based on the multivariant state in martensite. It confirms that the training process can be considered as a counterproductive process to martensitic transformation in which the shear processes associated with the rigid body rotations are restored. In other words, the training procedure that leads to a one-variant state in martensite can be regarded as a process that reverses the individual rotations obtained as a result of the aforementioned transformation. Therefore, the way in which the single variant of martensite is achieved (training process) does not affect the final orientation being consistent with the austenitic orientation. For these reasons, the orientation process in the austenite phase is more effective separately on the orientation relationship or the transformation mode. On the other hand, proper orientation of single crystalline materials maximizes Schmid factor, increasing the given strain and decreasing the twinning stress. This has a great impact on the functional properties of these alloys, which are mainly based on highly mobile twin boundaries.

Acknowledgement

The work was carried out within the project 2018/29/B/ST8/02343 of the National Science Centre of Poland.

REFERENCES

[1] K. Ullakko, J.K. Huang, C. Kantner, R.C. O'Handley, V.V. Kokorin, Appl. Phys. Lett. **69** (1996). DOI: https://doi.org/10.1063/1.117637

[2] E. Pagounis, R. Chulist, M.J. Szczerba, M. Laufenberg, Appl. Phys. Lett. **105**, 052405 (2014). DOI: https://doi.org/10.1063/1.4892633

[3] E. Pagounis, M.J. Szczerba, R. Chulist, M. Laufenberg, Appl. Phys. Lett. **107**, 152407 (2009). DOI: https://doi.org/10.1063/1.4933303

[4] A. Sozinov, N. Lanska, A. Soroka, W. Zou, Appl. Phys. Lett. **102**, 021902 (2013). DOI: https://doi.org/10.1063/1.4775677

[5] F. Chen, B. Tian, L. Li, Y. Zheng, Phys. Scr. T129 **227** (2007). DOI: https://doi.org/10.1088/0031-8949/2007/T129/051

[6] D.M. Liu, Z.H. Nie, Y.D. Wang, Y.D. Liu, G. Wang, Y. Ren, L. Zuo, Metall. Mater. Trans. A **39**, 466 (2008). DOI: https://doi.org/10.1007/s11661-007-9435-8

[7] B. Tian, F. Chen, Y. Liu, Y.F. Zheng, Mater. Lett. **62**, 2851 (2008). DOI: https://doi.org/10.1016/j.matlet.2008.01.071

[8] I. Suorsa, J. Tellinen, K. Ullakko, E. Pagounis, Appl. Phys. **95**, 8054 (2004). DOI: https://doi.org/10.1063/1.1711181

[9] N. Sarawate, M. Dapino, Phys. Lett. **88**, 121923 (2006). DOI: https://doi.org/10.1063/1.2189452

[10] I. Karaman, B. Basaran, H.E. Karaca, A.I. Karsilayan, Y.I. Chumlyakov, Appl. Phys. Lett. **90**, 172505 (2007). DOI: https://doi.org/10.1063/1.2721143

[11] H.E. Karaca, I. Karaman, B. Basaran, Y. Ren, Y.I. Chumlyakov, H.J. Maier, Adv. Funct. Mater. **19**, 983 (2009). DOI: https://doi.org/10.1002/adfm.200801322

[12] S. Barker, E. Rhoads, P. Lindquist, M. Vreugdenhil, P. Müllner, J. Med. Device **10**, 041009 (2016). DOI: https://doi.org/10.1115/1.4034576

[13] N.M. Bruno, C. Ciocanel, H.P. Feigenbaum, A. Waldauer, Smart Mater. Struct. **21**, 094018 (2012). DOI: https://doi.org/10.1088/0964-1726/21/9/094018

[14] D.C. Dunand, P. Müllner, Adv. Mater **23**, 216 (2011). DOI: https://doi.org/10.1002/adma.201002753

[15] U. Gaitzsch, S. Roth, B. Rellinghaus, L. Schultz, J. Magn. Mater. **305**, 275 (2006). DOI: https://doi.org/10.1016/j.jmmm.2006.01.017

[16] U. Gaitzsch, J. Romberg, M. Pötschke, S. Roth, P. Müllner, Scr. Mater. **65**, 679 (2011). DOI: https://doi.org/10.1016/j.scriptamat.2011.07.011

[17] M. Pötschke, U. Gaitzsch, S. Roth, B. Rellinghaus, L. Schultz, J. Magn. Magn. Mater. **316**, 383 (2007). DOI: https://doi.org/10.1016/j.jmmm.2007.03.032

[18] K. Ullakko, Y. Ezer, A. Sozinov, G. Kimmel, P. Yakovenko, V. Lindroos, Scr. Mater. **44**, 475 (2001). DOI: https://doi.org/10.1016/S1359-6462(00)00610-2

[19] U. Gaitzsch, M. Pötschke, S. Roth, B. Rellinghaus, L. Schultz, Acta Mater. **57**, 365 (2009). DOI: https://doi.org/10.1016/j.actamat.2008.09.017

[20] C. Hürrich, S. Roth, H. Wendrock, M. Pötschke, D. Cong, B. Rellinghaus, L. Schultz, J. Phys. Conf. Ser. **303**, 012080 (2011). DOI: https://doi.org/10.1088/1742-6596/303/1/012080

[21] N. Scheerbaum, O. Heczko, J. Liu, D. Hinz, L. Schultz, O. Gutfleisch, New J. Phys. **10**, 073002 (2008). DOI: https://doi.org/10.1088/1367-2630/10/7/073002

[22] V. Zhukova, V. Rodionova, L. Fetisov, A. Grunin, A. Goikhman, A. Torcunov, A. Aronin, G. Abrosimova, A. Kiselev, N. Perov, A. Granovsky, T. Ryba, S. Michalik, IEEE Trans. Magn. **50**, 4 (2014).

[23] M. Chmielus, X.X. Zhang, C. Witherspoon, D.C. Dunand, P. Müllner, Nature Materials **8**, 863 (2009). DOI: https://doi.org/10.1038/nmat2527

[24] S.Y. Yu, A.J. Gu, S.S. Kang, S.J. Hu, Z.C. Li, S.T. Ye, H.H. Li, J.J. Sun, R.R. Hao, J. Alloys Compd. **681**, 1 (2016). DOI: http://doi.org/10.1016/j.jallcom.2016.04.249

[25] D.M. Liu, Z.H. Nie, Y.D. Wang, Y.D. Liu, G. Wang, Y. Ren, L. Zuo, Metall. Mater. Trans. A **39**, 466 (2008). DOI: https://doi.org/10.1007/s11661-007-9435-8

[26] B. Tian, F. Chen, Y. Liu, Y.F. Zheng, Mater. Lett. **62**, 2851 (2008). DOI: https://doi.org/10.1016/j.matlet.2008.01.071

[27] T.D. Hatchard, J.S. Thorne, S.P. Farrell, R.A. Dunlap, J. Phys.: Condensed. Matter. **20**, 445205 (2008). DOI: https://doi.org/10.1088/0953-8984/20/44/445205

[28] V.A. Chernenko, E. Cesari, J. Pons, C. Segui, J. Mater. Research **15**, 1496 (2000). DOI: https://doi.otg/10.1557/JMR.2000.0215

[29] O. Heczko, P. Svec, D. Janickovic, K. Ullakko, IEEE Transactions on Magnetics **38**, 2841 (2002). DOI: https://doi:10.1109/TMAG.2002.802471

[30] N.V. Rama Rao, R. Gopalan, V. Chandrasekaran, K.G. Suresh, J. Alloys Compd. **478**, 59 (2009). DOI: https://doi.org/10.1016/j.jallcom.2008.12.015

[31] J. Gutiérrez, J.M. Barandiarán, P. Lázpita, C. Seguí, E. Cesari Sens, Actuators A: Phys. **129**, 163 (2006). DOI: https://doi.org/10.1016/j.sna.2005.11.035

[32] R. Chulist, P. Czaja, Scripta Mater. **189**, 106 (2020). DOI: https://doi.org/10.1016/j.scriptamat.2020.08.007

[33] R. Chulist, K. Nalepka, A. Sozinov, Int. J. Plast. **126**, 102628 (2020).

[34] A. Wójcik, R. Chulist, P. Czaja, M. Kowalczyk, P. Zackiewicz, N. Schell, W. Maziarz, Acta Mater. **219**, 117237 (2021). DOI: https://doi.org/10.1016/j.actamat.2021.117237

[35] R. Chulist, M. Faryna, M.J. Szczerba, Acta Mater. **103**, 836-843 (2016). DOI: https://doi.org/10.1016/j.actamat.2015.11.007

[36] R. Chulist, M. Faryna, M.J. Szczerba, Journal of Materials Science **51**, 10943-10948 (2016). DOI: https://doi.org/10.1007/s10853-016-0306-9

[37] R. Chulist, P. Czaja, T. Tokarski, I. Kuksgauzen, Y.I. Chumlyakov, Int. J. Plast. **114**, 63-71 (2019).